Journal of New Materials for Electrochemical Systems 16, 253-256 (2013)

Short Communication

Study of a Novel Cathode Material for Magnesium Secondary Battery

Jian-zhi SUN

Key Laboratory of Coordination Chemistry and Functional Materials in Universiities of Shandong (Dezhou University),
Shandong Dezhou 253023, P. R. China;

Received: June 23, 2013, Accepted: August 03, 2013, Available online: October 30, 2013

Abstract: *Orthosilicate $MgNiSiO_4$ materials were prepared by sol-gel approach and a molten salt method. The preparation process had a profound effect on the morphology of the materials. As a new cathode for magnesium secondary battery, the material shows a reversible Mg^{2+} intercalation-deintercalation process. Preliminary electrochemical data indicated that the $MgNiSiO_4$ prepared by a molten salt method had a higher peak current, a larger discharge capacity and a better cyclability compared with the $MgNiSiO_4$ prepared by sol-gel approach. The results show that $MgNiSiO_4$ could be a potential cathode material for high-energy magnesium secondary battery.*

Keywords: Magnesium secondary battery; Orthosilicate; Synthetic methods; Electrochemical performance

1. INTRODUCTION

Following the achievements in the field of lithium-ion battery, there have been more and more attempts over the years to develop magnesium secondary battery, due to its natural abundance, relatively low price, and higher expected safety[1-3]. One of the encountered difficulties is the low mobility of Mg^{2+} in the host lattice, since Mg^{2+} has high surface charge density. Consequently, fast Mg^{2+} transport in the intercalation host is required at ambient temperature.

The magnesium secondary battery had not been paying much attention because of mainly two problems [4, 5]. One is passivating surface film grown on Mg, which obstructs reversible electrochemical reaction. Another is the difficulty of insertion and diffusion in the cathode material for divalent magnesium ion. It is so far well known that Mg^{2+} insertion into ion transfer hosts proceeds slowly owing to the strong polarization effect of small and divalent Mg^{2+} ion compared with Li^+ or Na^+ and only a small discharge capacity has been reported for magnesium insertion cathode. As a result, it is necessary to realize fast Mg^{2+} transport in the host in addition to other requirements as practical cathode materials for magnesium battery [6].

Recently, the orthosilicate materials caught the attention of the scientists due to high reversible capacity, and it has been suggested that $MgMSiO_4$ (M=Mn, Fe, Co) can store large amounts of charge per unit mass as cathode materials for magnesium secondary battery via a highly reversible redox reaction [7-11]. Here, we propose that $MgNiSiO_4$ is feasible as potential cathode materials for magnesium batteries. In this study, $MgNiSiO_4$ was prepared by sol-gel approach and a molten salt method, and the Mg^{2+} intercalation/deintercalation process was investigated as a new cathode material for magnesium secondary battery.

2. EXPERIMENTAL

2.1. Preparation of $MgNiSiO_4$

$MgNiSiO_4$ materials were synthesized by sol-gel approach and a molten salt method. For the sol-gel approach, First, the starting materials of magnesium acetate ($MgAc_2 \cdot 4H_2O$) and nickel acetate ($NiAc_2 \cdot 4H_2O$) in a stoichiometric ratio were dissolved in alcohol with magnetic stirring. After a clear solution formed, and then the Ethyl silicate ($C_8H_{20}O_4Si$) is added by dropwise into the resulting solution while increasing the temperature to 60 ~ 90 °C and keep stirring 18-24 h. The gel was decomposed at 100 °C in vacuum drying oven for 12 h, and the obtained product was ground, and sintered at 800 °C for 24 h under conditions of argon shield. The final product was named SG-$MgNiSiO_4$.

For the molten-salt method, KCl (melting point is 780 °C) was used as as flux after drying overnight at 120°C under vacuum to provide a liquid-state reaction environment when the reaction temperature was increased above 780 °C. Magnesium oxide (MgO), nickel carbonate ($NiCO_3$) and silicon dioxide (SiO_2, 15–20 nm)

---

*To whom correspondence should be addressed: Email: jianzhisun@163.com and KCl were mixed using a mortar and pestle for a few minutes and poured into a corundum crucible at a molar ratio of Mg:Co:Si:KCl = 1:1:1:4. It was then dried at 120 °C for 3 h under vacuum to remove the water content from the mixture. After that, the mixture was immediately transferred to a tube furnace and heated in an Ar atmosphere at 400 °C for 3 h to remove oxalate groups, followed by the final firing at 1000 °C for 6 h, then cooling to room temperature naturally. Finally, the product was washed three times with deionized water by centrifugation three times to remove any remaining salt and dried at 100 °C for 2 h under vacuum. The product was named MS-$MgNiSiO_4$.

2.2. Characterization and Electrochemical Measurements

2.2.1. XRD

The X-ray diffraction(XRD) was performed at room temperature on a Rigaku D/max-3B X-Ray diffractometer, the X-ray beam was nickel-filtered Cu *Ka* (λ=0.15406 nm) radiation operated at 40 kV and 30 mA; and the data were collected from 5 ° to 80 °(2*θ*) at a scanning rate of 5 °/min.

2.2.2. Electrochemical measurements

Electrochemical Mg-ion intercalation performances of the samples were evaluated in Mg test cells. The cathode materials were prepared by mixing the samples with acetylene black and polytetrafluoroethylene (PTFE) with a weight ratio of 85:10:5 in ethanol to ensure homogeneity. After the ethanol was evaporated, the mixture was rolled into a sheet, and the sheet was cut into circular strips of 8 mm in diameter. The strips were then dried at 100 °C for 10 h. Magnesium metal was used as an anode. The standard electrolyte solutions comprised THF and Mg salts (0.25 M) of the general formula, Mg $(AlCl_2BuEt)_2$, a reaction product of $MgBu_2$ and $AlCl_2Et$ in a 1:2 ratio. Their preparation has already been reported elsewhere [12]. The cell assembly was carried out in a controlled environment using a glove box under an argon atmosphere. Then, the cell was maintained at 20 °C for 24 h in order to establish the equilibrium state of the electrodes with the electrolyte. Cyclic Voltammetry (CV) measurements were performed on a Reference 600 multichannel workstation manufactured by USA AMETEK, Inc. Galvanostatic charge/discharge was recorded with a Land battery measurement system (Wuhan, China) with the cutoff voltage of 2.1/0.5 V, at room temperature.

3. RESULTS AND DISCUSSION

3.1. Characterization of sample

XRD patterns of samples prepared via the sol-gel method and the molten-salt method are shown in Fig. 1. The diffraction peaks of all the samples were well-crystallized and in full accordance with the standard $MgNiSiO_4$ phase (standard database JCPDS card No: 84-1990) with ordered olivine structure indexed by orthorhombic Pbnm(62). Compared with those of MS-$MgNiSiO_4$, the main diffraction peaks of SG-$MgNiSiO_4$ slightly broadened, and the relative peak intensity was lower, which was probably due to the polycrystalline character and smaller particle size of the materials. The comparison showed that the magnesium-nickel-silicate phase could be more facilely obtained at a moderate temperature and the reaction period by the molten-salt method (1200 °C for 8 h) than the sol-gel method (1200 °C for 24 h).

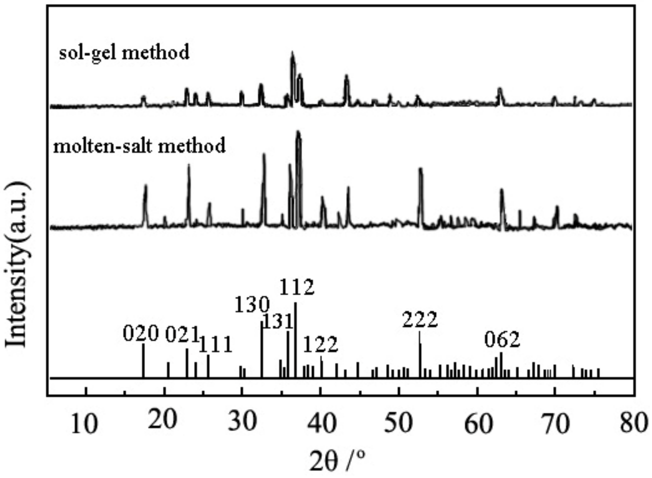

Figure 1. The XRD patterns of $MgNiSiO_4$ sample

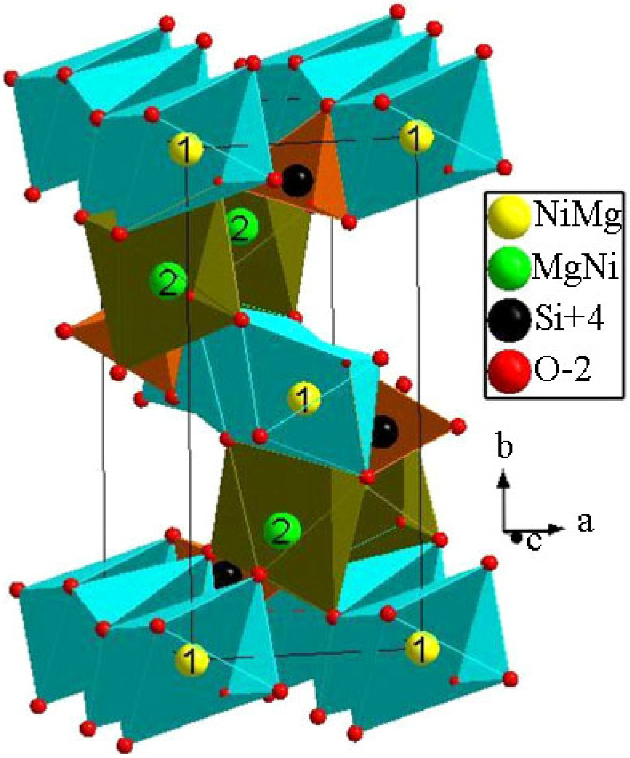

Figure 2. Ordered crystal structure of natural olivine $MgNiSiO_4$ in polyhedral representation. Alternate Mg1Ni1 and Mg2Ni2 are shown as spheres [11]

In natural olivine $MgNiSiO_4$, the Mg and Ni ions were located in the center of the MO6 units, while the alternating sites of Ni1Mg1 (represented as balls with 1) and Mg2Ni2 (represented as balls with 2) were located within the octahedrons. Si sites were located within the tetrahedrons, while oxygen atoms were located in the corners[13]. The crystal structure revealed mixed site occupation of the same octahedral sites by Mg and Ni atoms with different atomic

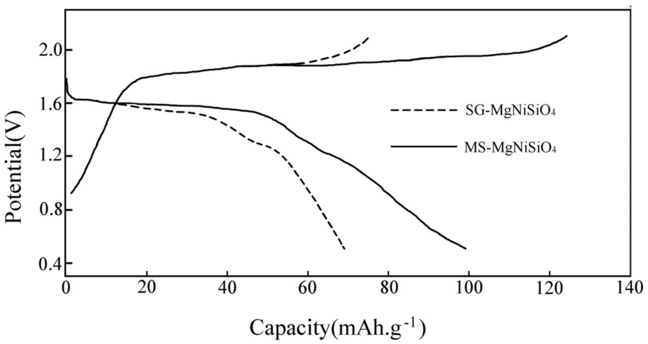

Figure 3. Typical charge/discharge curves of the $MgNiSiO_4$ electrode at 5 mA·g^{-1} at 25 ℃

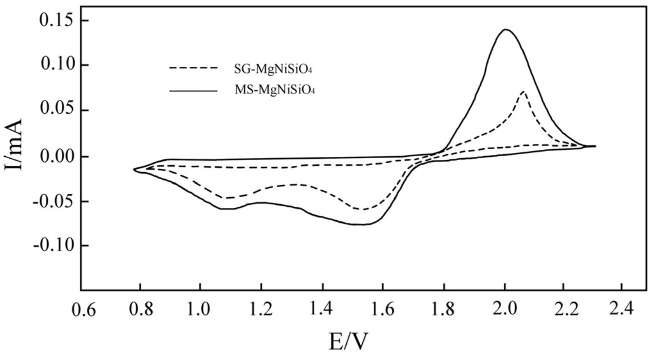

Figure 4. Cyclic voltammetry (CV) curves of $MgNiSiO_4$ electrodes measured at a low scan rate of 0.01 mv·s^{-1}.

site occupied fractions. In other words, there were two positions for the Mg atoms to occupy in the crystal structure with different geometrical circumstances.

3.2. Electrochemical properties

The initial galvanostatic discharge/charge curves for SG-$MgNiSiO_4$ and MS-$MgNiSiO_4$ test cells are shown in Figure 3, measured at a current density of 5 mA·g^{-1} in the potential range of 2.1-0.5 V at 25 °C. Both cells exhibit two discharge plateaus around 1.6 and 1.2 V. For MS-$MgNiSiO_4$, the discharge voltage reached approximately 1.6 V versus Mg, and the capacity was 97.8 mAh·g^{-1} (compared with 68.1 mAh·g^{-1} for SG-$MgNiSiO_4$), which was 59.5% of the theoretical value (164.5 mAh·g^{-1}). The large capacity loss may arise from parasitic processes, such as electrolyte decomposition of the electrode material. Furthermore, the slow ion diffusion rate and low electronic conductivity in the materials also contributed to the irreversibility of the reaction. It should be mentioned that the Mg^{2+} insertion/extraction potentials for the $MgNiSiO_4$ samples were similar to those for $MgCoSiO_4$, $MgFeSiO_4$ and $Mg_{1.03}Mn_{0.97}SiO_4$. It was different from that of Li^+ in $LiMPO_4$ (M = Mn, Fe, Co and Ni), for which the redox potentials were dependent on the transition metals[14]. The lower anodic stability of the Mg $(AlCl_2EtBu)_2$/THF electrolyte may limit the entire extraction of Mg^{2+} from $MgNiSiO_4$.

The initial CV curves are shown in Figure 4 for the SG-$MgNiSiO_4$ and MS-$MgNiSiO_4$ electrodes. There are two pairs of redox peaks marked for both electrodes, in agreement with the charge/discharge curves (Figure 4), which can be attributed to the intercalation and de-intercalation reactions. That is to say, the Mg^{2+} intercalation into the magnesium deficient positive electrode proceeds via two stages, which is in good agreement with the analysis of its crystal structure. As mentioned above, there were two kinds of occupation sites for the Mg atoms, M1 and M2, in the $MgNiSiO_4$ structure. According to the distribution of the total capacity for the magnitude of the two peaks, the peaks of 1.6 V could be attributed to the de-intercalation/intercalation of Mg^{2+} from/into the M1 sites while the peaks of 1.2 V corresponds to Mg insertion at M2 sites.

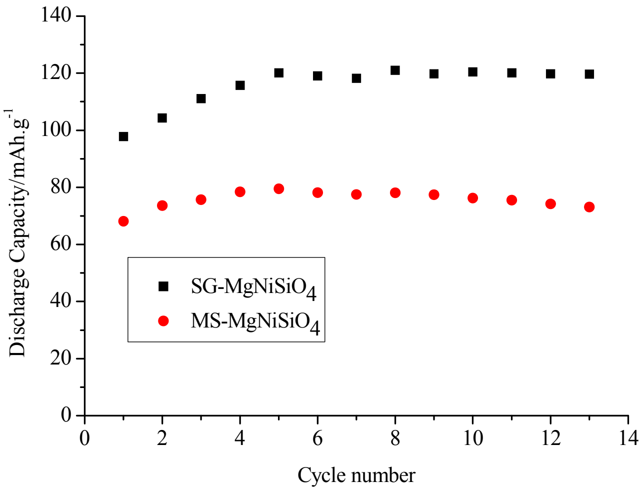

Figure 5. Cyclic performances of $MgNiSiO_4$ tested at 10 mA·g^{-1} at 25 °C.

In Figure 4 there are some apparent differences between the two curves. The current density of the MS-$MgNiSiO_4$ electrode is higher than that of the SG-$MgNiSiO_4$ electrode. For the coin-type cell systems the electrode can approximately be regarded as a flat one, and the peak current density is represented as follows: $i_p=2.6\times10^5 n^{3/2} C_0 D^{1/2} v^{1/2}$, where n is the number of electrons transferred per molecule during the intercalation, C_0 is the concentration of magnesium ions, D is the diffusion coefficient of magnesium ions, and v is the scan rate [15]. Since $i_p \propto D^{1/2}$, the diffusion coefficient of magnesium ions has been higher in the MS-$MgNiSiO_4$ electrode than in the SG-$MgNiSiO_4$ electrode.

Fig. 5 shows the variation of discharge capacities versus cycle number at a current density of 10 mA·g^{-1}. It is interesting that MS-$MgNiSiO_4$ and SG-$MgNiSiO_4$ exhibited an activation process during the initial cycles due to the gradual infiltration of electrolyte into the electrodes[12]. The discharge capacity of SG -$MgNiSiO_4$ increases from 68.1 mAh·g^{-1} in the first cycle to 79.5 mAh·g^{-1} in the 5th cycle (compared with from 97.8 mAh·g^{-1} to 120.1 mAh·g^{-1} for SG-$MgNiSiO_4$). Compared with SG-$MgNiSiO_4$, MS-$MgNiSiO_4$ clearly showed higher discharge capacities and better cyclic ability.

4. CONCLUSION

$MgNiSiO_4$ materials prepared by sol-gel approach and a molten salt method exhibited distinct and reversible electrochemical intercalation behavior. Preliminary electrochemical data demonstrated that MS-$MgNiSiO_4$ showed a higher peak current, a larger discharge capacity and a better cyclability compared with SG-$MgNiSiO_4$. The discharge capacity of MS-$MgNiSiO_4$ is 120.1 $mAh \cdot g^{-1}$ in the 5th cycle at a current density of 10 $mA \cdot g^{-1}$. An optimization of both the material structure and the electrolyte compatibility is necessary to increase the specific capacity and cycle performance.

5. ACKNOWLEDGMENTS

This work was supported by a grant from the National Natural Foundation of China (No. 20971018) and the Natural Science Foundation of Shandong (No. ZR2009FQ027).

REFERENCES

[1] J. Giraudet, D. Claves, K. Guérin, M. Dubois, A. Houdayer, F. Masin, A. Hamwia, J. Power Sources, 173, 592 (2007).

[2] R. Shahid, S. Shinya, Y. Shu, M. Masaru, Solid State Ionics, 225, 542 (2012).

[3] T. Kakibe, J. Hishii, N. Yoshimoto, M. Egashira, M. Morita, Journal of Power Sources, 203, 195 (2012).

[4] T. Kakibe, N. Yoshimoto, M. Egashira, M. Morita, Electrochem. Commun., 12, 1630 (2010).

[5] Y.S. Guo, J. Yang, Y.N. Nuli, J.L. Wang, Electrochem. Commun., 12, 1671 (2010).

[6] G.S. Suresh, M.D. Levi, D. Aurbach, Electrochimica Acta, 53, 3889 (2008).

[7] Z.Z. Feng, J. Yang, Y.N. Nuli, J.L. Wang, J. Power Sources, 184, 604 (2008).

[8] Y.N. Nuli, J. Yang, Y.S. Li, J.L. Wang, Chem. Commun., 46, 3794 (2010).

[9] Y.N. Nuli, Y.P. Zheng, F. Wang, J. Yang, A.I. Minett, J.L. Wang, J. Chen. Electrochemistry Communications, 13, 1143 (2011).

[10]Y. Li, Y.N. Nuli, J. Yang, Y. Tuhudahong, J.L. Wang, Chinese Science Bulletin, 56, 386 (2011).

[11]Y.P. Zheng, Y.N. Nuli, Q. Chen, Y. Wang, J. Yang, J.L. Wang, Electrochimica Acta, 66, 75 (2012).

[12]O. Chusid, Y. Gofer, H. Gizbar, Y. Vestfrid, E. Levi, D. Aurbach, I. Riech. Adv. Mater., 15, 627 (2003).

[13]R. Rinaldi, G.D. Gatta, G. Artioli, K.S. Knight, C.A. Geiger, Phys. Chem. Miner., 32, 655 (2005).

[14]C.A.J. Fisher, P.V.M. Hart, M.S. Islam, Chem. Mater., 20, 5907 (2008).

[15]H. Liu, L.J. Fu, H.P. Zhang, J. Gao, C. Li, Y.P. Wu, H.Q. Wu, Electrochem. Solid-State Lett., 9, A529 (2006).